microbiology research

MDPI

Article

Environmental and Clinical Spread of MDR *Acinetobacter baumannii*: A Genomic Epidemiology Investigation

Alice Caramaschi [1,*], Marianna Farotto [2], Marta Mellai [3,4], Francesco Favero [3,5], Davide Corà [3,5], Paolo Bottino [6,*], Christian Leli [6], Lidia Ferrara [6], Chiara Bazzano [1], Silvio Collani [1], Valeria Bonato [7], Andrea Rocchetti [6], Marinella Bertolotti [8], Annalisa Roveta [8], Antonio Maconi [8] and Elisa Bona [1,3]

1 Department for Sustainable Development and Ecological Transition, University of Eastern Piedmont, 13100 Vercelli, Italy; chiara.bazzano@uniupo.it (C.B.); silvio.collani@uniupo.it (S.C.); elisa.bona@uniupo.it (E.B.)
2 Research and Innovation Department (DAIRI), ASL Alessandria, 15121 Alessandria, Italy; mfarotto@aslal.it
3 University Center for Translational Research on Autoimmune and Allergic Diseases (UPO-CAAD), University of Eastern Piedmont, 28100 Novara, Italy; marta.mellai@uniupo.it (M.M.); francesco.favero@uniupo.it (F.F.); davide.cora@uniupo.it (D.C.)
4 Department of Health Sciences, University of Piemonte Orientale, 28100 Novara, Italy
5 Department of Translational Medicine, University of Eastern Piedmont, 28100 Novara, Italy
6 Microbiology and Virology Laboratory, IRCCS Azienda Ospedaliero-Universitaria "SS. Antonio e Biagio e Cesare Arrigo", 15121 Alessandria, Italy; christian.leli@ospedale.al.it (C.L.); lidia.ferrara@ospedale.al.it (L.F.); arocchetti@ospedale.al.it (A.R.)
7 Department of Anaesthesia and Intensive Care, IRCCS Azienda Ospedaliero-Universitaria "SS. Antonio e Biagio e Cesare Arrigo", 15121 Alessandria, Italy; vbonato@ospedale.al.it
8 Research Training Innovation Infrastructure, Research and Innovation Department (DAIRI), IRCCS Azienda Ospedaliero-Universitaria "SS. Antonio e Biagio e Cesare Arrigo", 15121 Alessandria, Italy; mbertolotti@ospedale.al.it (M.B.); aroveta@ospedale.al.it (A.R.); amaconi@ospedale.al.it (A.M.)
* Correspondence: alice.caramaschi@uniupo.it (A.C.); paolo.bottino@ospedale.al.it (P.B.)

Abstract

During the COVID-19 pandemic, healthcare systems experienced significant disruption, increasing the risk of multidrug-resistant (MDR) pathogen transmission. *Acinetobacter baumannii*, a critical-priority MDR pathogen, is known for its ability to persist in hospital environments and rapidly acquire resistance. To investigate the genomic characteristics, antimicrobial resistance determinants, and phylogenetic relationships of outbreak-associated *Acinetobacter baumannii* isolates, whole-genome sequencing (WGS) and comparative genomic analyses on 24 clinical and environmental strains collected during the COVID-19 period were performed. Twenty-four *A. baumannii* isolates collected between August 2020 and February 2021 from clinical and environmental samples were analyzed by WGS. All isolates displayed an MDR phenotype, with uniform resistance to carbapenems and aminoglycosides, and preserved colistin susceptibility. One environmental strain showed extreme drug resistance. WGS confirmed medium-quality genome assemblies and the clonal spread of a single *A. baumannii* lineage. Most resistance genes, including *OXA-23*, *ADC-type* β-lactamases, and *ade* efflux pumps, were chromosomally encoded and shared across all isolates. Plasmid-mediated resistance genes were variably distributed. This outbreak of MDR *A. baumannii* was driven by the clonal dissemination of a genomically stable lineage. Combined genomic and epidemiological analyses underscore the importance of integrated surveillance and environmental decontamination to prevent the spread of MDR pathogens.

Keywords: *Acinetobacter baumannii*; multidrug resistance; whole-genome sequencing; hospital outbreak; carbapenem resistance; international clone 2; genomic epidemiology

Academic Editor: Hector M. Mora-Montes

Received: 28 May 2026
Revised: 16 July 2026
Accepted: 22 July 2026
Published: 3 August 2026

1. Introduction

Healthcare-associated infections (HAIs) continue to pose a major public health challenge, especially when caused by multidrug-resistant organisms (MDROs). These infections lead to increased morbidity, mortality, and healthcare costs due to limited treatment options and prolonged hospital stays [1,2]. Among MDROs, *Acinetobacter baumannii* is a critical pathogen included in the WHO priority list due to its capacity to acquire resistance to most available antibiotics and to persist in hospital environments [3].

Carbapenem-resistant *A. baumannii* (CRAB) is a major concern in European healthcare settings. Recent surveillance data show that over 80% of *A. baumannii* isolates are resistant to carbapenems, with the highest prevalence reported in Southern Europe, notably Italy and Greece [4]. This trend is associated with the increased use of broad-spectrum antimicrobials and suboptimal infection prevention and control (IPC) measures, especially in intensive care units (ICUs) [5,6].

The success of *A. baumannii* as a nosocomial pathogen is due not only to its resistance profile but also to several virulence traits, including biofilm formation, outer membrane proteins facilitating host cell adhesion, and enzymes promoting tissue damage and immune evasion [7–9]. The colonization of skin and mucosa, including among healthcare personnel, may contribute to unnoticed transmission and persistence in hospital wards [10].

Patients with prolonged hospitalization, ICU admission, invasive procedures or underlying conditions such as trauma, burns, or immunosuppression are at increased risk of infection [11,12]. In this context, the rapid and accurate characterization of *A. baumannii* clusters is essential to implement timely control measures.

Whole-genome sequencing (WGS) has become a powerful tool in outbreak investigations, allowing for the high-resolution analysis of clonal relatedness, resistance genes and transmission routes [11,13,14]. The integration of WGS with epidemiological data is increasingly used in national and international surveillance frameworks to guide containment strategies and support antimicrobial stewardship efforts.

This study aimed to investigate a nosocomial cluster of CRAB detected across multiple departments of a tertiary care hospital in Alessandria, Italy. By combining epidemiological investigation with WGS, we sought to: (i) assess the clonal relatedness of the isolates; (ii) identify potential transmission routes; and (iii) characterize the genetic determinants of antimicrobial resistance. The findings were intended to inform targeted infection prevention and control actions and contribute to the ongoing national surveillance of MDROs.

2. Materials and Methods

2.1. Study Setting and Isolate Collection

This study was conducted in accordance with the ethical principles outlined in the Declaration of Helsinki and relevant national and institutional regulations.

All bacterial isolates were collected as part of routine microbiological surveillance activities and anonymized prior to analysis. No personal or identifiable patient data were used, and no additional biological sampling was performed for research purposes. This study therefore did not require informed consent according to national legislation on retrospective observational studies.

This research was carried out in collaboration with the University of Eastern Piedmont, and the Research and Innovation Department (DAIRI, ASL Alessandria) complies with institutional biosafety and data protection policies. Twenty-four *A. baumannii* isolates were collected at Microbiology Laboratory of the IRCCS Azienda Ospedaliero-Universitaria of Alessandria "SS. Antonio e Biagio e Cesare Arrigo", Research and Innovation Department (DAIRI-AOU AL), during a nosocomial outbreak that occurred between 2020 and 2021, coinciding with the COVID-19 pandemic. Isolates were obtained from clinical

and surgical materials in eight wards: Cardiac Surgery (CCHI), General Surgery (2CH), Intensive Care Unit (CR), Infectious Diseases (MINF), Emergency Department (JDEA), Coronary Unit (UCJ), Pneumology (PN), and Thoracic Surgery (CHTO) (Table S1). Samples were stored at −80 °C until processing. Bacterial identification was performed using the VITEK2 automated system (bioMérieux, Marcy-l'Étoile, France), following standard laboratory protocols.

2.2. Antimicrobial Susceptibility Determination and Validation

The minimum inhibitory concentrations (MICs) of antimicrobial agents against *Acinetobacter baumannii* isolates were initially determined using the automated VITEK 2 system (bioMérieux, Marcy-l'Étoile, France), according to the manufacturer's instructions. Briefly, pure bacterial colonies grown on appropriate agar medium were suspended in sterile saline solution and adjusted to the turbidity required for VITEK 2 antimicrobial susceptibility testing. The standardized suspension was used to inoculate the appropriate VITEK 2 AST card for Gram-negative bacteria, which was then loaded into the instrument for automated incubation, reading, and MIC determination. The MIC values obtained were interpreted according to EUCAST clinical breakpoints for *Acinetobacter* spp. The results were used to define the antimicrobial susceptibility profile of each *A. baumannii* isolate, and selected MICs were further assessed using the MICRONAUT/MCN6 broth microdilution-based system (MERLIN Diagnostika GmbH, Borheim, Germany). For this purpose, isolates were cultured overnight on Columbia blood agar, and a bacterial suspension equivalent to 0.5 McFarland was prepared in sterile 0.9% saline solution. An aliquot of 50 µL of this suspension was inoculated into 11.5 mL of Müller–Hinton broth and thoroughly mixed. Subsequently, 100 µL of the inoculated broth was dispensed into each well of a MICRONAUT MIC plate (MERLIN Diagnostika GmbH, Borheim, Germany). Plates were sealed with adhesive film and incubated at 37 °C for 18 h. Optical density was measured using a TECAN SUNRISE microplate reader (TECAN Trading AG, Männedorf, Switzerland), and minimum inhibitory concentrations (MICs) were determined using MCN6 software (MERLIN Diagnostika GmbH), according to the manufacturer's instructions. MIC values were interpreted according to EUCAST clinical breakpoints v.10.0, 2020, where available. For tigecycline, MIC values were reported descriptively and were not assigned to susceptible or resistant categories, as no EUCAST clinical breakpoints are available for tigecycline against *A. baumannii*.

2.3. Whole-Genome Sequencing

Strains were grown on Müller–Hinton agar and incubated overnight in Müller–Hinton broth at 37 °C. Genomic DNA was extracted using the DNeasy® UltraClean® Microbial Kit (QIAGEN, Milan, Italy) according to the manufacturer's instructions. DNA concentration was quantified using the Qubit™ dsDNA HS assay kit (Invitrogen, Singapore), while DNA purity was assessed by NanoDrop (Thermo Fisher Scientific, Monza, Italy) spectrophotometry. Samples were accepted for library preparation when they contained sufficient double-stranded DNA to meet the Illumina Nextera XT input requirement and showed purity ratios compatible with downstream sequencing. Specifically, DNA was normalized to 0.2 ng/µL, corresponding to 1 ng total input DNA, and samples with A260/280 ratios of approximately 1.8–2.0 and A260/230 ratios preferably ≥1.8 were considered suitable for library preparation. Samples not meeting these quality criteria were re-quantified and, where necessary, further purified before proceeding to library construction. Library preparation was performed using the Illumina Nextera XT DNA Library Preparation Kit according to the manufacturer's instructions. For each sample, a specific index mix was prepared by combining two unique indexes to allow for sample multiplexing. The indexing

PCR was performed under the following thermal conditions: 72 °C for 3 min and 95 °C for 30 s, followed by amplification cycles consisting of 95 °C for 10 s, 55 °C for 30 s and 72 °C for 30 s, with a final extension at 72 °C for 5 min and hold at 10 °C. PCR products were purified using Agencourt AMPure XP beads, according to the manufacturer's instructions. Briefly, bead–sample mixtures were incubated at room temperature for 2 min and processed following the recommended washing and elution steps.

Fragment size distribution was assessed using the High Sensitivity D5000 kit on a 4200 TapeStation system (Agilent Technologies, Waldbronn, Germany). Libraries were prepared for normalization by mixing ladder and samples with Sample Buffer in optical tubes, followed by centrifugation at 671× *g* at 20 °C for 1 min. Based on fragment size and concentration, libraries were normalized and pooled. Shotgun sequencing of the 6 pM library pool was performed on an Illumina MiSeq platform (Illumina, Milan, Italy) using the MiSeq Reagent Kit v3. PhiX Control v3 (Illumina, San Diego, CA, USA) was included as an internal sequencing control.

2.4. Bioinformatic Analysis

Raw reads were quality-checked using FastQC v0.11.5 and trimmed with Trimmomatic v0.36 to remove low-quality sequences (Phred score < 30) [15]. Reads were assembled using SPAdes v3.15.5 in two steps [16]. First, assemblies were generated using the --plasmid and --careful options to reconstruct plasmid sequences. These plasmid contigs were indexed with Bowtie2 [17] and reads mapping on them were removed from the original dataset using custom Perl scripts. A second SPAdes run (with --careful only) was thus performed on the remaining filtered dataset of raw reads to reconstruct the chromosomal genome. Genome completeness and contamination were evaluated using CheckM2 v1.0.1 [18].

Open reading frames (ORFs) were predicted with Prodigal v2.6.3 [19], retaining only complete proteins. Functional annotation was carried out with EggNOG-mapper v2.1.12 using the eggNOG 5.0.2 database [20]. Annotation parameters included DIAMOND-based alignment with minimum thresholds for identity (40%) and coverage (20%). Antibiotic resistance genes (ARGs) were identified using Resistance Gene Identifier (RGI) software v6.0.3 from the Comprehensive Antibiotic Resistance Database (CARD) [21]. Heatmaps representing antibiotic resistance genes identified by the RGI tool were produced in an R environment using the "pheatmap" and "RcolorBrewer" packages. To assess phylogenetic relationships, 24 reconstructed genomes were compared with *A. baumannii* reference genomes downloaded from the ATCC Genomes Portal and NCBI. Phylogenetic reconstruction was performed including the 24 outbreak-associated *A. baumannii* genomes and selected reference genomes. Outgroups were selected to include both a closely related intrageneric reference within *Acinetobacter* and more distant Gram-negative representatives, including *Pseudomonas* spp., to support tree rooting and provide broader phylogenetic context. The *Pseudomonas* genomes were used exclusively as distant outgroups and were not considered epidemiologically related to the outbreak isolates. All genomes were annotated using the same pipeline and aligned at the protein level using PhyloPhlAn v3.1.68 with default parameters https://huttenhower.sph.harvard.edu/phylophlan/ [22]. The resulting phylogenetic tree was visualized using FigTree v1.4.4 (http://tree.bio.ed.ac.uk/software/figtree/, accessed on 10 July 2026). To further investigate the phylogenetic distance among the 24 reconstructed genomes, the allelic distances of these genomes were computed by performing a cgMLST analysis using ChewBBACA software v3.4.2 [23], setting the standard *A. baumannii* available on the cgMLST.org Nomenclature Server (NCS) website as a schema [24]. Allelic distances among our reconstructed genomes and the *A. baumannii* reference species also present in the phylogenetic tree were also calculated. To reduce assembly-related missing loci and to compare more properly different species, only informative loci for

at least 95% of the samples were retained. An allelic distance matrix was imported into PHYLOViZ 2.0 [25], where a graph of distances was calculated with the application of the geoBURST Full MST algorithm. The resulting graph was imported into Cytoscape Java version 1.8.0 [26] to improve graphical representation.

3. Results

3.1. Phenotypic Characterization of Acinetobacter baumannii Isolates

The 24 *Acinetobacter baumannii* isolates were collected at Alessandria Hospital between August 2020 and February 2021 from both clinical and environmental sources (Table S1). Overall, 21 isolates were recovered from clinical specimens, including 12 from blood cultures and nine from bronchoalveolar lavage samples, while three isolates originated from environmental surfaces. The Reanimation Centre accounted for the largest proportion of isolates (n = 11), comprising five blood culture isolates, five bronchoalveolar lavage isolates, and one environmental isolate recovered from a personal protective equipment cart. Five isolates were associated with the Intensive Cardiac Surgery Unit, including two blood culture isolates, one bronchoalveolar lavage isolate, and two environmental isolates obtained from a medication trolley and a patient bedside. The remaining isolates were collected from the Infectious Diseases Unit (n = 2, both blood cultures), the Emergency Department (n = 2, both blood cultures), General Surgery (n = 1, blood culture), the Coronary Unit (n = 1, bronchoalveolar lavage), Pneumology (n = 1, bronchoalveolar lavage), and Thoracic Surgery (n = 1, bronchoalveolar lavage). This distribution documents the occurrence of the outbreak across multiple hospital wards and supports the involvement of both patient-related and environmental reservoirs. All isolates displayed a multidrug-resistant (MDR) phenotype (Tables S1 and S2), with high-level resistance to carbapenems (meropenem MIC $\geq$ 2 mg/L; all strains classified as resistant) and aminoglycosides (amikacin MIC $\geq$ 32 mg/L in 23/24 isolates). Most isolates also exhibited resistance to gentamicin, ciprofloxacin, and trimethoprim/sulfamethoxazole. Notably, colistin susceptibility was preserved in all isolates that showed low colistin MIC values, with observed MICs $\leq$ 0.5 mg/L, and were therefore classified as susceptible according to EUCAST clinical breakpoints for *Acinetobacter* spp. (S $\leq$ 2 mg/L; R > 2 mg/L) v.10.0, 2020. Two strains isolated from environmental surfaces (Bau 22 and 23) showed a broader resistance profile, including resistance to piperacillin/tazobactam and fosfomycin, and presented MIC values above clinical breakpoints for most tested antibiotics. Strain Bau 23 displayed extreme drug resistance, with MICs $\geq$ 256 for two antimicrobial agents. Tigecycline MICs are reported as observed MIC values only. No categorical interpretation was assigned for tigecycline, because validated EUCAST clinical breakpoints for tigecycline against *A. baumannii* are not available. Therefore, tigecycline results were not included in the calculation of susceptibility/resistance rates.

The antimicrobial susceptibility profiles obtained using the in-house MIC platform were highly consistent with those reported by broth microdilution and EUCAST interpretation, showing near-complete categorical agreement across all antibiotics tested. No systematic discrepancies were observed, supporting the analytical reliability of the MIC approach.

3.2. Whole-Genome Reconstruction

Whole-genome sequencing (WGS) data were deposited in the NCBI BioProject under accession PRJNA983793 (https://www.ncbi.nlm.nih.gov/bioproject/PRJNA983793, accessed on 21 May 2026), within the study monitoring the spread of *Acinetobacter* spp. in the high-risk units of Alessandria Hospital. The primary objective of this analysis was to reconstruct bacterial genomes and characterize their genomic similarity and protein-

coding gene repertoire, with particular emphasis on antibiotic resistance determinants. Genome assembly was performed using the SPAdes pipeline, followed by quality control and annotation procedures.

Assembly quality was evaluated using CheckM2, and completeness and contamination metrics were visualized in a scatter plot at the chromosomal level (Figure 1A). All reconstructed genomes showed medium assembly quality, with contamination scores consistently below 0.4% and completeness values exceeding 75%, while some of them showed also high assembly quality > 90% and contamination < 5%. Species assignment was subsequently assessed by calculating Mash distances against the Genome Taxonomy Database. For all assemblies, the closest reference genome corresponded to *A. baumannii* (Figure 1B).

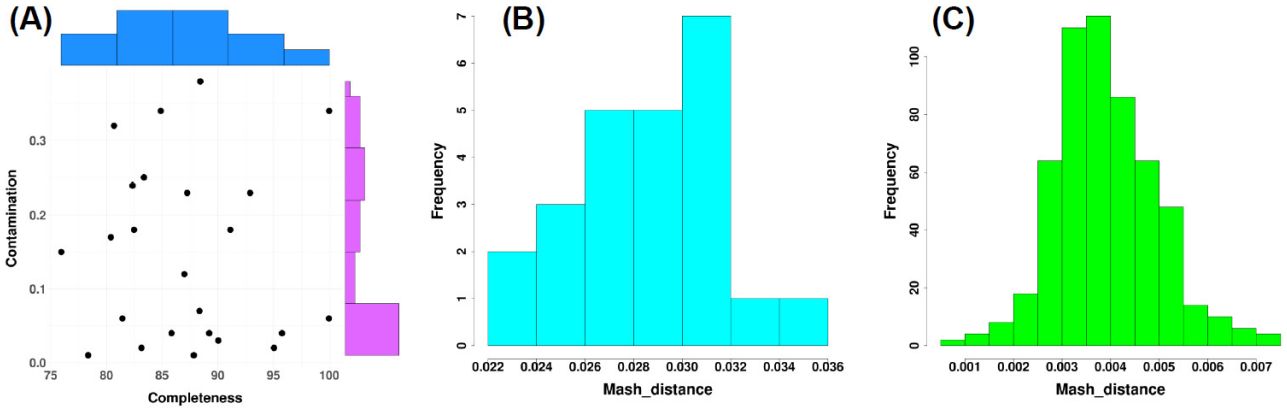

Figure 1. (**A**) A scatter plot reporting the completeness and contamination of each reconstructed genome as calculated by Checkm2 software. (**B**) A histogram reporting the distribution of the Mash distances between each reconstructed genome and the *Acinetobacter baumannii* reference from the Genome Taxonomy Database release 214. (**C**) A histogram reporting the distribution of the Mash distances between each pair of reconstructed genomes.

To determine whether the reconstructed genomes represented multiple strains or a single clonal lineage, pairwise Mash distances were computed among all chromosomal assemblies. As shown in Figure 1C, all genome pairs exhibited Mash distances below 0.007. This finding was corroborated by FastANI analysis, which revealed average nucleotide identity values greater than 99% across all pairwise comparisons (Table S3). Collectively, these results support the presence of a highly homogeneous genomic population consistent with a single strain rather than multiple distinct lineages.

To further contextualize genomic relatedness among the reconstructed isolates, pairwise distance relationships in a network representation (Figure 2) were visualized. The graph highlights a highly compact genomic structure centred on isolate Bau1, which acts as a hub connecting all other outbreak genomes. The distances between Bau1 and the remaining clinical isolates were minimal, ranging from one to three units, consistent with the low Mash distances and high ANI values observed previously. This tight clustering supports the interpretation of a clonally related population circulating within the hospital setting.

In contrast, comparisons with publicly available *Acinetobacter sp.* reference genomes revealed markedly greater distances. The closest external reference strain showed distances exceeding 180 units, while additional reference genomes were separated by values above 200 units. This pronounced separation indicates that, despite belonging to the same species, the outbreak isolates form a highly homogeneous genomic cluster distinct from broader population diversity. Together, these findings reinforce the evidence for a single, closely

related outbreak lineage and confirm the robustness of the genomic similarity analyses reported above.

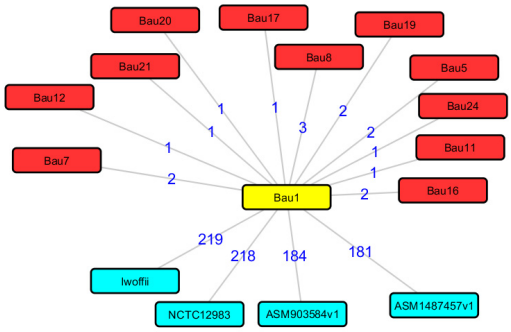

Figure 2. A graph reporting the allelic distance among each reconstructed genome and a series of reference *A. baumannii* genomes as calculated by the geoBURST Full MST algorithm. The Bau1 yellow hub node represents the best reconstructed *A. baumannii*. Red nodes represent other *A. baumannii* species. Cyan nodes represent the *Acinetobacter sp.* reference species (Iwoffii: *Acinetobacter iwoffii;* NCTC12983: *Acinetobacter calcoaceticus;* ASM903584v1: *A. baumannii;* ASM1487457v1: *A. baumannii*) In Bau1, the collapse of Bau1, Bau2, Bau3, Bau4, Bau6, Bau9, Bau10, Bau13, Bau14, Bau15, Bau18, Bau22, Bau23 and reconstructed genomes is represented since the allelic distance among these reconstructed genomes is 0.

The functional characterization of the reconstructed genomes was conducted by predicting protein-coding genes with Prodigal and annotating them using EggNOG for both chromosomal and plasmid sequences.

Antibiotic resistance genes were specifically investigated using the Resistance Gene Identifier (RGI). The RGI analysis (Figure 3) indicated that most resistance determinants were located on chromosomal DNA rather than plasmid sequences.

Additional assembly metrics are provided in Tables S3 and S4 for chromosomal and plasmid sequences, respectively.

Chromosomal assembly statistics (Table S4) revealed variability in fragmentation, with contig counts ranging from 140 to 775 per genome. Genome sizes were consistent with reference *A. baumannii* genomes, spanning 2.91–3.74 Mbp (mean ~3.29 Mbp), and G + C content remained uniform (38.9–39.3%). Predicted coding sequences ranged from 2591 to 3481 per genome, with coding densities generally exceeding 79% and reaching up to 86.9%. Average gene lengths were stable across isolates (914–942 bp), whereas average contig lengths varied substantially, reflecting differences in assembly continuity. Overall, these metrics confirm the suitability of the WGS data for downstream phylogenetic and comparative genomic analyses.

Plasmid assembly statistics (Table S5) demonstrated marked heterogeneity in plasmid content among the 24 isolates.

The number of plasmid contigs ranged from 8 to 92, with total assembly sizes between 32.4 kbp and 996.9 kbp. Plasmid G + C content (37.6–41.3%) was broadly consistent with chromosomal values. Predicted coding sequences ranged from 34 to 892, with coding densities exceeding 80% in most assemblies. Several isolates exhibited particularly high coding proportions (>85%), with average gene lengths near 1 kbp. Variation in contig length indicated diverse plasmid architectures. These plasmid assemblies provide a framework for investigating mobile genetic elements, including resistance and virulence determinants that may contribute to outbreak persistence and dissemination (Table S6).

In order to investigate the quality of our reconstruction, we decided to also focus on the quality of the reconstructed proteome: phylogenetic relationships among reconstructed

genomes were inferred by comparing chromosomal proteomes, with tree visualization performed using FigTree (Figure 4).

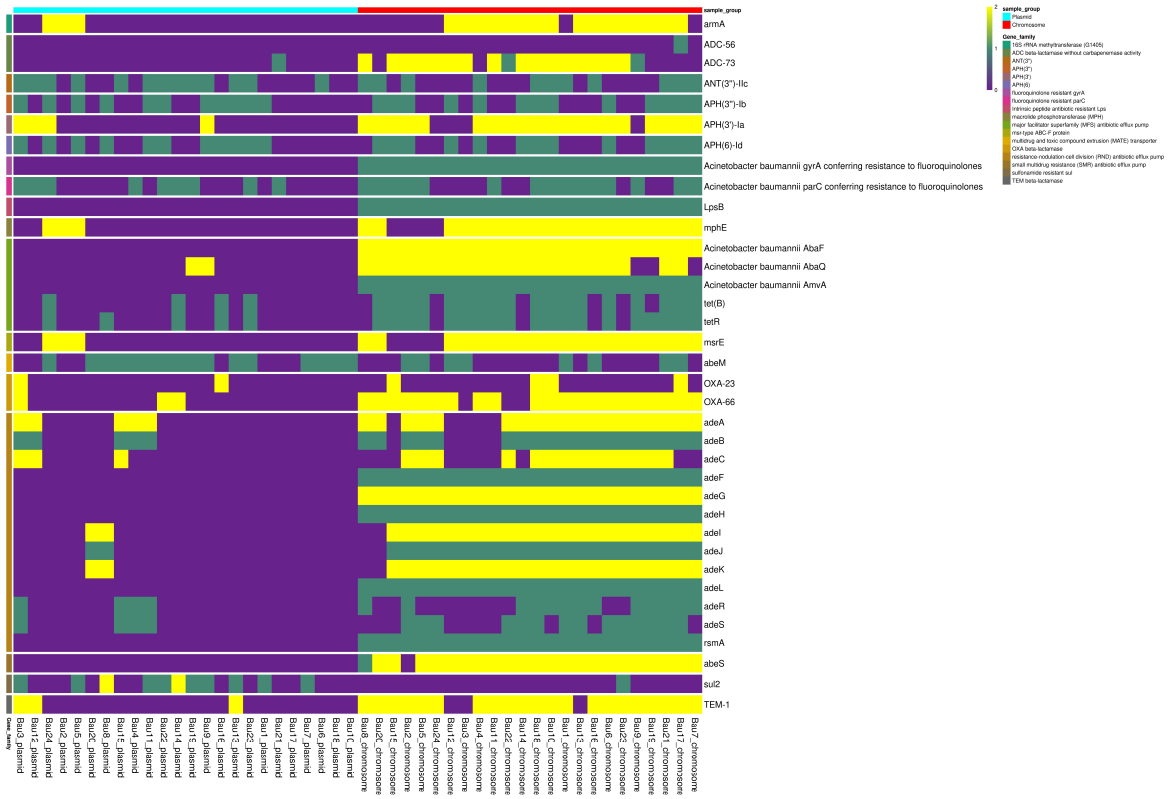

Figure 3. A heatmap representation of the AMR-associated determinants/loci displayed as individual rows across the *A. baumannii* genomes analyzed by the RGI analysis pipeline. Each column represents an individual reconstructed genome, while rows correspond to specific resistance genes or gene families. Colour coding indicates the detection status of each gene: yellow denotes confirmed presence, purple indicates absence, and green represents partial detection or low-confidence matches based on sequence similarity thresholds. The colour bar at the top summarizes the location of the identified genes: light blue—plasmid; red—chromosome. Entries corresponding to *gyrA* and *parC* indicate quinolone resistance-associated target loci identified by the annotation pipeline. These loci should not be interpreted as acquired resistance genes, as fluoroquinolone resistance is mediated by specific QRDR mutations.

Table S7 shows the results of the MLST analysis. All the reconstructed genomes were fully compatible with a Pasteur/Oxford ST "abaumannii_2" reference. The "Alleles" column reports potential differences in some reference alleles.

3.3. Distribution of Resistance and Efflux Genes in Outbreak Isolates

The analysis of antimicrobial resistance (AMR)-associated determinants and efflux pump components across the 24 *A. baumannii* genomes revealed a complex resistome architecture characterized by a conserved chromosomal backbone and a more variable plasmid-associated component (Figure 3). Overall, 36 AMR-associated determinants/loci were identified when each annotated heatmap row was counted separately. These included β-lactamase genes (*OXA-23*, *OXA-66*, *TEM-1*, *ADC-56*, *ADC-73*), aminoglycoside resistance determinants (*armA*, *APH(3′)-Ia*, *ANT(3″)-IIc*, *APH(3″)-Ib*, *APH(6)-Id*), macrolide resistance genes (*msrE*, *mphE*), tetracycline resistance genes (*tet(B)*, *tetR*), and the sulphonamide resistance gene *sul2*. Additional AMR-associated loci included *LpsB*, *rsmA*, and multiple efflux pump genes or regulators, such as components of the *AdeABC*, *AdeFGH* and *AdeIJK* systems, together with *adeR*, *adeS*, *adeL*, *AbaQ*, *AbaF*, *AmvA*, *AbeM* and *AbeS*. In addition, *gyrA* and

parC were detected as quinolone resistance-associated target loci by the annotation pipeline. However, these genes are chromosomal housekeeping genes, and quinolone resistance depends on specific QRDR mutations rather than on gene presence alone; therefore, they were not interpreted as acquired resistance genes.

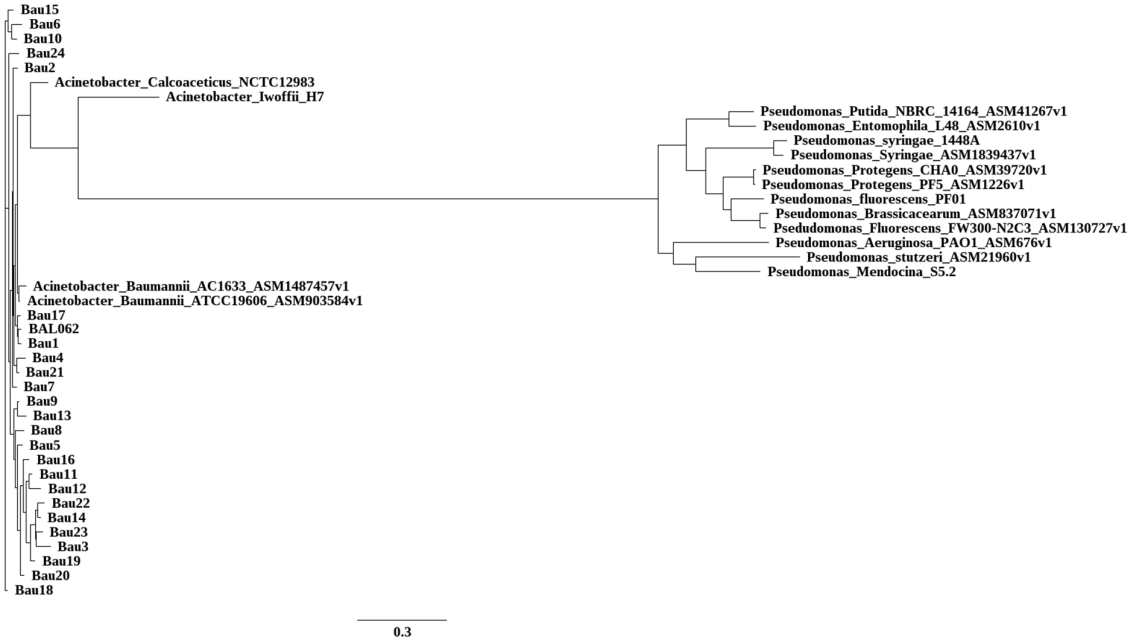

Figure 4. A phylogenetic tree of several reference bacteria and our reconstructed genome samples of *Acinetobacter baumannii*. The phylogenetic tree was built starting from the predicted proteins of each genome. The phylogenetic tree includes the 24 outbreak-associated *A. baumannii* genomes, selected *Acinetobacter* reference genomes, and distant Gram-negative outgroups represented by *Pseudomonas* spp. The *Pseudomonas* sequences were included only to provide an external rooting/reference group and do not imply epidemiological or taxonomic proximity to the outbreak isolates.

Chromosomally encoded determinants, including *OXA-66*, ADC variants, fluoroquinolone-associated target determinants and several multidrug efflux systems, were broadly conserved across the isolate collection. In contrast, plasmid-associated resistance determinants showed a more variable distribution. For instance, *OXA-23* and *armA* were detected in a subset of plasmid compartments, consistent with their role in carbapenem and aminoglycoside resistance dissemination via mobile genetic elements. Plasmid-associated *TEM-1* and *sul2* were identified in multiple but not all isolates, suggesting sporadic acquisition events. Efflux systems are discussed here at the functional system or operon level, whereas Figure 3 reports individual annotated gene components as separate rows. Together, these findings suggest that both the vertical transmission of conserved chromosomal resistance determinants and horizontal acquisition of plasmid-associated AMR genes contributed to the resistome diversity observed during the outbreak.

4. Discussion

This study provides an integrated phenotypic and genomic investigation of a nosocomial outbreak of *A. baumannii* that occurred during the COVID-19 pandemic at a tertiary care hospital in Northern Italy. The outbreak involved both clinical and environmental isolates, all of which exhibited a multidrug-resistant (MDR) phenotype, with high-level resistance to carbapenems, aminoglycosides, and several other antimicrobial classes. These findings are consistent with the established resistance profile of high-risk international

clones of *A. baumannii* IC2 that have been spreading across European healthcare systems over the past decade [27,28].

The resistance determinants identified in our isolates, particularly *OXA-23* and *armA*, are among the most clinically relevant genes associated with carbapenem and aminoglycoside resistance, respectively [5,27,29,30]. Their detection in both plasmid and chromosomal compartments highlights the complex interplay between clonal expansion and horizontal gene transfer in shaping the resistome of outbreak strains. While all isolates showed colistin MICs consistent with susceptibility according to the interpretive criteria applied, tigecycline MIC values were higher in a subset of strains, including the extensively drug-resistant (XDR) environmental isolate BAU 23. These tigecycline data were interpreted descriptively, as no validated EUCAST clinical breakpoints are available for tigecycline against *A. baumannii* [31].

Whole-genome reconstruction revealed a clonal origin of the outbreak, with all isolates belonging to a single phylogenetic lineage. This finding is supported by Mash and ANI metrics and suggests that dissemination likely occurred within the hospital environment rather than through multiple external introductions. The simultaneous recovery of isolates from clinical samples and inanimate surfaces—including PPE carts, trolleys, and bedside areas—highlights the importance of environmental contamination in sustaining transmission chains [32]. During the COVID-19 pandemic, the extraordinary pressure on healthcare systems, including staffing shortages, the increased use of invasive procedures, and challenges in implementing standard infection control protocols, may have facilitated the persistence and spread of MDR pathogens such as *A. baumannii* [12].

A major strength of this study is the separate reconstruction and analysis of chromosomal and plasmid genomes, which revealed important differences in gene content and resistance gene localization. Chromosomal resistance determinants—such as *OXA-66*, *ADC-type* β-lactamases, and efflux pump operons (*adeABC*, *adeFGH*, *adeIJK*)—were consistently present across isolates, supporting their role in intrinsic resistance. Conversely, plasmid-borne resistance genes showed heterogeneous distribution. *OXA-23*, *armA*, *TEM-1*, and *sul2* were found only in a subset of plasmids, reflecting recent or intermittent acquisition events through horizontal gene transfer (HGT) [33–35]. Plasmid assemblies were highly variable in structure and content, ranging from small, low-density elements to complex, gene-rich plasmids with high coding density, reinforcing their role as key vectors in the mobilization of resistance traits [36].

These findings underline the dual nature of resistance dissemination in *A. baumannii*: the vertical transmission of core chromosomal mechanisms and horizontal acquisition of mobile elements. The ability of *A. baumannii* to stably integrate plasmid-derived resistance genes, combined with its environmental persistence and biofilm-forming capacity, makes it a particularly formidable pathogen in hospital settings [36].

Beyond the reconstruction of the outbreak dynamics, this study provides an operational framework for the application of genomic surveillance to infection prevention and control. The integration of whole-genome sequencing data with clinical, epidemiological and environmental information can help identify possible transmission routes, detect environmental reservoirs and distinguish clonal spread from sporadic contamination events. From this perspective, the aim of this study was to promote the introduction of integrated genomic surveillance, encompassing both clinical isolates and environmental samples, within the hospital setting. This approach may support hospital management and infection control teams in planning targeted interventions to limit the dissemination of multidrug-resistant microorganisms. Such interventions may include extraordinary environmental decontamination procedures, the reinforcement of cleaning protocols for high-touch surfaces and shared equipment, the revision of nursing and patient care procedures, and

enhanced microbiological monitoring in critical wards. Therefore, genomic epidemiology should not be considered only a retrospective investigative tool but also a practical resource to guide timely, evidence-based containment strategies against multidrug-resistant pathogens. Our results have relevant implications for hospital infection control policies. First, they demonstrate the need for routine genomic surveillance, which enables the early detection of outbreak strains, characterization of transmission routes, and monitoring of resistance evolution. Second, the presence of highly resistant strains in environmental reservoirs suggests that surface disinfection and environmental monitoring should be considered key components of outbreak containment strategies, particularly during pandemic scenarios when resources are stretched, and standard procedures may be deprioritized [12].

The network-based genomic distance analysis suggests that the outbreak isolates form a highly homogeneous cluster, consistent with the circulation of a dominant *A. baumannii* lineage (belonging to the international clone IC2) within the hospital setting. While genomic similarity alone cannot definitively reconstruct transmission chains, the compact clustering pattern, together with the low Mash distances and high ANI values observed across isolates, is compatible with recent shared ancestry and localized dissemination. Similar genomic signatures have been described in hospital-associated *A. baumannii* outbreaks, where clonal expansion reflects sustained persistence in clinical environments characterized by high antibiotic pressure and repeated opportunities for cross-transmission [37].

Importantly, the predominance of antibiotic resistance determinants encoded within the chromosomal compartment suggests that resistance traits are stably maintained within this lineage rather than being driven primarily by transient plasmid acquisition. The chromosomal integration of resistance genes has been associated with the long-term adaptation of epidemic *A. baumannii* clones to healthcare environments, promoting persistence under selective antimicrobial pressure [28,38]. In this context, the observed genomic uniformity may reflect the success of a well-adapted resistant lineage rather than ongoing diversification through horizontal gene transfer. Nevertheless, the presence of heterogeneous plasmid architectures indicates that mobile genetic elements remain an important reservoir of accessory traits that could influence fitness, virulence, or additional resistance profiles [39].

Taken together, these findings support a scenario in which a genetically stable, antibiotic-resistant clone circulates within high-risk hospital units, likely facilitated by ecological persistence and selective pressure rather than rapid genomic diversification. However, given the inherent limitations of genomic inference without detailed epidemiological metadata, these patterns should be interpreted cautiously. Whole-genome similarity provides strong evidence of relatedness but does not by itself resolve the directionality or timing of transmission events. The integration of genomic surveillance with infection control data remains essential to fully characterize transmission dynamics and to guide targeted containment strategies.

This study has some limitations. First, it was conducted within a single tertiary care hospital, which may limit the generalizability of the findings to other healthcare settings. Second, while whole-genome sequencing provided high-resolution insight into clonal relationships and resistance determinants, short-read sequencing may have constrained the complete reconstruction of large or complex plasmids. Third, clinical metadata, including patient outcomes and antibiotic exposure history, were not systematically available, preventing a comprehensive assessment of the clinical impact of specific resistance profiles. Finally, environmental sampling was limited to selected hospital wards and timepoints, which may have underestimated the true extent of environmental contamination. Despite these limitations, the integration of genomic and epidemiological analyses provides a robust framework for understanding the dynamics of *A. baumannii* dissemination and

reinforces the importance of environmental surveillance during periods of healthcare strain such as the COVID-19 pandemic.

5. Conclusions

In conclusion, this study documents the clonal dissemination of an MDR *A. baumannii* lineage during the COVID-19 pandemic, supported by both chromosomally encoded resistance mechanisms and heterogeneous plasmid-mediated gene acquisition. It highlights the critical role of genomic epidemiology in outbreak investigation and the necessity of integrating molecular data with routine microbiology and infection control to contain the spread of MDR pathogens in healthcare environments.

Supplementary Materials: The following supporting information can be downloaded at https://www.mdpi.com/article/10.3390/microbiolres17080150/s1, Table S1: Antimicrobial susceptibility profiles of 24 *Acinetobacter baumannii* isolates collected from clinical and environmental sources at Alessandria Hospital, Italy (August 2020–February 2021). Table S2: Antimicrobial susceptibility profiles of *Acinetobacter baumannii* isolates according to EUCAST criteria; Table S3: Pairwise Average Nucleotide Identity (ANI) values among 24 Acinetobacter baumannii isolates collected during a nosocomial outbreak at Alessandria Hospital, Italy (August 2020–February 2021). Table S4: A table reporting the stats of each reconstructed genome (chromosomal). Table S5: A table reporting the stats of each reconstructed genome (plasmid). Table S6: A table reporting the complete annotation of the predicted proteins for each chromosome and plasmid. Table S7: The results of the MLST analysis.

Author Contributions: A.C.: investigation, validation, formal analysis, software, data curation, visualization and writing—original draft; M.F.: formal analysis and writing—review and editing; M.M.: formal analysis and writing—review and editing; F.F.: software, data curation and writing—review and editing; D.C.: data curation and writing—review and editing; P.B.: data curation and writing—review and editing; C.L.: data curation and writing—review and editing; L.F.: formal analysis; C.B.: investigation, validation, formal analysis, software, data curation, visualization and writing—original draft; S.C.: formal analysis, data curation, visualization and writing—original draft; V.B.: writing—review and editing; A.R. (Andrea Rocchetti): investigation, data curation and writing—review and editing; M.B.: writing—review and editing; A.R. (Annalisa Roveta): investigation and writing—review and editing; A.M.: writing—review and editing; E.B.: project administration, data curation, writing—original draft and writing—review and editing. All authors have read and agreed to the published version of the manuscript.

Funding: This study was conducted with the partial funding from Azianda Ospedaliera Universitaria "Santi Antonio e Biagio e Cesare Arrigo", Alessandria, Italy.

Institutional Review Board Statement: Not applicable. This study was conducted in accordance with the ethical principles outlined in the Declaration of Helsinki and relevant national and institutional regulations. All bacterial isolates were collected as part of routine microbiological surveillance activities and anonymized prior to analysis. No personal or identifiable patient data were used, and no additional biological sampling was performed for research purposes.

Informed Consent Statement: Not applicable. This study therefore did not require informed consent according to national legislation on retrospective observational studies. This research was carried out in collaboration with the University of Eastern Piedmont, and the Research and Innovation Department (DAIRI, ASL Alessandria) complies with institutional biosafety and data protection policies.

Data Availability Statement: The authors shared the raw data (fastq files) in the public NCBI repository at the following link: (https://www.ncbi.nlm.nih.gov/bioproject/PRJNA983793).

Acknowledgments: The authors acknowledge the support of Facility di Integrative Genomics (CAAD, Università del Piemonte Orientale) and the Facility of Bioinformatics and thank Mellai and Favero for

technical assistance. This research was partially funded by "Azienda Ospedaliero-Universitaria "SS Antonio e Biagio e Cesare Arrigo", Alessandria, Italy"-"*Monitoraggio della diffusione di Acinetobacter sp. in diversi reparti a rischio*".

Conflicts of Interest: The authors declare no conflicts of interest.

References

1. Ali, S.; Birhane, M.; Bekele, S.; Kibru, G.; Teshager, L.; Yilma, Y.; Ahmed, Y.; Fentahun, N.; Assefa, H.; Gashaw, M.; et al. Healthcare Associated Infection and Its Risk Factors among Patients Admitted to a Tertiary Hospital in Ethiopia: Longitudinal Study. *Antimicrob. Resist. Infect. Control* **2018**, *7*, 2. [CrossRef]
2. Magill, S.S.; Edwards, J.R.; Bamberg, W.; Beldavs, Z.G.; Dumyati, G.; Kainer, M.A.; Lynfield, R.; Maloney, M.; McAllister-Hollod, L.; Nadle, J.; et al. Multistate Point-Prevalence Survey of Health Care-Associated Infections. *N. Engl. J. Med.* **2014**, *370*, 1198–1208. [CrossRef]
3. World Health Organization (Ed.) *Antimicrobial Resistance: Global Report on Surveillance*; World Health Organization: Geneva, Switzerland, 2014.
4. Antimicrobial Resistance in the EU/EEA (EARS-Net)—Annual Epidemiological Report for 2023. 2023. Available online: https://www.amr-insights.eu/antimicrobial-resistance-in-the-eu-eea-ears-net-annual-epidemiological-report-for-2023/ (accessed on 21 May 2026).
5. Kyriakidis, I.; Vasileiou, E.; Pana, Z.D.; Tragiannidis, A. *Acinetobacter baumannii* Antibiotic Resistance Mechanisms. *Pathogens* **2021**, *10*, 373. [CrossRef] [PubMed]
6. Marino, A.; Augello, E.; Bellanca, C.M.; Cosentino, F.; Stracquadanio, S.; La Via, L.; Maniaci, A.; Spampinato, S.; Fadda, P.; Cantarella, G.; et al. Antibiotic Therapy Duration for Multidrug-Resistant Gram-Negative Bacterial Infections: An Evidence-Based Review. *Int. J. Mol. Sci.* **2025**, *26*, 6905. [CrossRef] [PubMed]
7. Eze, E.C.; Chenia, H.Y.; El Zowalaty, M.E. Acinetobacter Baumannii Biofilms: Effects of Physicochemical Factors, Virulence, Antibiotic Resistance Determinants, Gene Regulation, and Future Antimicrobial Treatments. *Infect. Drug Resist.* **2018**, *11*, 2277–2299. [CrossRef] [PubMed]
8. Geisinger, E.; Isberg, R.R. Interplay Between Antibiotic Resistance and Virulence During Disease Promoted by Multidrug-Resistant Bacteria. *J. Infect. Dis.* **2017**, *215*, S9–S17. [CrossRef] [PubMed]
9. Uppalapati, S.R.; Sett, A.; Pathania, R. The Outer Membrane Proteins OmpA, CarO, and OprD of *Acinetobacter baumannii* Confer a Two-Pronged Defense in Facilitating Its Success as a Potent Human Pathogen. *Front. Microbiol.* **2020**, *11*, 589234. [CrossRef] [PubMed]
10. Gurieva, T.V.; Bootsma, M.C.; Bonten, M.J. Decolonization of Patients and Health Care Workers to Control Nosocomial Spread of Methicillin-Resistant *Staphylococcus aureus*: A Simulation Study. *BMC Infect. Dis.* **2012**, *12*, 302. [CrossRef] [PubMed]
11. Shi, J.; Mao, X.; Sun, F.; Cheng, J.; Shao, L.; Shan, X.; Zhu, Y. Epidemiological Characteristics and Antimicrobial Resistance of Extensively Drug-Resistant *Acinetobacter baumannii* in ICU Wards. *Microbiol. Spectr.* **2025**, *13*, e0261924. [CrossRef] [PubMed]
12. da Silva, R.T.P.; Rocha, I.V.; Dantas, T.F.; Silva, J.D.S.; da Costa Júnior, S.D.; de Oliveira Luz, A.C.; Moreno, M.; Leal-Balbino, T.C.; Araújo Lima, A.V.; da Silva, E.G.; et al. Emergence and Spread of Resistant and Biofilm-Forming *Acinetobacter baumannii* in Critically Ill COVID-19 Patients. *Microb. Pathog.* **2024**, *197*, 107078. [CrossRef] [PubMed]
13. Higgins, P.G.; Prior, K.; Harmsen, D.; Seifert, H. Development and Evaluation of a Core Genome Multilocus Typing Scheme for Whole-Genome Sequence-Based Typing of *Acinetobacter baumannii*. *PLoS ONE* **2017**, *12*, e0179228. [CrossRef] [PubMed]
14. Quainoo, S.; Coolen, J.P.M.; van Hijum, S.A.F.T.; Huynen, M.A.; Melchers, W.J.G.; van Schaik, W.; Wertheim, H.F.L. Whole-Genome Sequencing of Bacterial Pathogens: The Future of Nosocomial Outbreak Analysis. *Clin. Microbiol. Rev.* **2017**, *30*, 1015–1063. [CrossRef] [PubMed]
15. Bolger, A.M.; Lohse, M.; Usadel, B. Trimmomatic: A Flexible Trimmer for Illumina Sequence Data. *Bioinformatics* **2014**, *30*, 2114–2120. [CrossRef] [PubMed]
16. Prjibelski, A.; Antipov, D.; Meleshko, D.; Lapidus, A.; Korobeynikov, A. Using SPAdes De Novo Assembler. *Curr. Protoc. Bioinform.* **2020**, *70*, e102. [CrossRef] [PubMed]
17. Langmead, B.; Salzberg, S.L. Fast Gapped-Read Alignment with Bowtie 2. *Nat. Methods* **2012**, *9*, 357–359. [CrossRef] [PubMed]
18. Chklovski, A.; Parks, D.H.; Woodcroft, B.J.; Tyson, G.W. CheckM2: A Rapid, Scalable and Accurate Tool for Assessing Microbial Genome Quality Using Machine Learning. *Nat. Methods* **2023**, *20*, 1203–1212. [CrossRef] [PubMed]
19. Hyatt, D.; Chen, G.-L.; Locascio, P.F.; Land, M.L.; Larimer, F.W.; Hauser, L.J. Prodigal: Prokaryotic Gene Recognition and Translation Initiation Site Identification. *BMC Bioinform.* **2010**, *11*, 119. [CrossRef] [PubMed]
20. Huerta-Cepas, J.; Szklarczyk, D.; Heller, D.; Hernández-Plaza, A.; Forslund, S.K.; Cook, H.; Mende, D.R.; Letunic, I.; Rattei, T.; Jensen, L.J.; et al. eggNOG 5.0: A Hierarchical, Functionally and Phylogenetically Annotated Orthology Resource Based on 5090 Organisms and 2502 Viruses. *Nucleic Acids Res.* **2019**, *47*, D309–D314. [CrossRef] [PubMed]

21. Alcock, B.P.; Huynh, W.; Chalil, R.; Smith, K.W.; Raphenya, A.R.; Wlodarski, M.A.; Edalatmand, A.; Petkau, A.; Syed, S.A.; Tsang, K.K.; et al. CARD 2023: Expanded Curation, Support for Machine Learning, and Resistome Prediction at the Comprehensive Antibiotic Resistance Database. *Nucleic Acids Res.* **2023**, *51*, D690–D699. [CrossRef] [PubMed]
22. Asnicar, F.; Thomas, A.M.; Beghini, F.; Mengoni, C.; Manara, S.; Manghi, P.; Zhu, Q.; Bolzan, M.; Cumbo, F.; May, U.; et al. Precise Phylogenetic Analysis of Microbial Isolates and Genomes from Metagenomes Using PhyloPhlAn 3.0. *Nat. Commun.* **2020**, *11*, 2500. [CrossRef] [PubMed]
23. Silva, M.; Machado, M.P.; Silva, D.N.; Rossi, M.; Moran-Gilad, J.; Santos, S.; Ramirez, M.; Carriço, J.A. chewBBACA: A Complete Suite for Gene-by-Gene Schema Creation and Strain Identification. *Microb. Genom.* **2018**, *4*, e000166. [CrossRef] [PubMed]
24. Jünemann, S.; Sedlazeck, F.J.; Prior, K.; Albersmeier, A.; John, U.; Kalinowski, J.; Mellmann, A.; Goesmann, A.; von Haeseler, A.; Stoye, J.; et al. Updating Benchtop Sequencing Performance Comparison. *Nat. Biotechnol.* **2013**, *31*, 294–296. [CrossRef] [PubMed]
25. Nascimento, M.; Sousa, A.; Ramirez, M.; Francisco, A.P.; Carriço, J.A.; Vaz, C. PHYLOViZ 2.0: Providing Scalable Data Integration and Visualization for Multiple Phylogenetic Inference Methods. *Bioinformatics* **2017**, *33*, 128–129. [CrossRef] [PubMed]
26. Shannon, P.; Markiel, A.; Ozier, O.; Baliga, N.S.; Wang, J.T.; Ramage, D.; Amin, N.; Schwikowski, B.; Ideker, T. Cytoscape: A Software Environment for Integrated Models of Biomolecular Interaction Networks. *Genome Res.* **2003**, *13*, 2498–2504. [CrossRef] [PubMed]
27. Abouelfetouh, A.; Mattock, J.; Turner, D.; Li, E.; Evans, B.A. Diversity of Carbapenem-Resistant *Acinetobacter baumannii* and Bacteriophage-Mediated Spread of the Oxa23 Carbapenemase. *Microb. Genom.* **2022**, *8*, 000752. [CrossRef] [PubMed]
28. Zarrilli, R.; Pournaras, S.; Giannouli, M.; Tsakris, A. Global Evolution of Multidrug-Resistant Acinetobacter Baumannii Clonal Lineages. *Int. J. Antimicrob. Agents* **2013**, *41*, 11–19. [CrossRef] [PubMed]
29. Hernández-González, I.L.; Mateo-Estrada, V.; Castillo-Ramirez, S. The Promiscuous and Highly Mobile Resistome of *Acinetobacter baumannii*. *Microb. Genom.* **2022**, *8*, 000762. [CrossRef] [PubMed]
30. Palmieri, M.; D'Andrea, M.M.; Pelegrin, A.C.; Perrot, N.; Mirande, C.; Blanc, B.; Legakis, N.; Goossens, H.; Rossolini, G.M.; van Belkum, A. Abundance of Colistin-Resistant, OXA-23- and ArmA-Producing *Acinetobacter baumannii* Belonging to International Clone 2 in Greece. *Front. Microbiol.* **2020**, *11*, 668. [CrossRef] [PubMed]
31. Sun, C.; Yu, Y.; Hua, X. Resistance Mechanisms of Tigecycline in *Acinetobacter baumannii*. *Front. Cell Infect. Microbiol.* **2023**, *13*, 1141490. [CrossRef] [PubMed]
32. Lerner, A.O.; Abu-Hanna, J.; Carmeli, Y.; Schechner, V. Environmental Contamination by Carbapenem-Resistant *Acinetobacter baumannii*: The Effects of Room Type and Cleaning Methods. *Infect. Control Hosp. Epidemiol.* **2020**, *41*, 166–171. [CrossRef] [PubMed]
33. Blackwell, G.A.; Hall, R.M. Mobilisation of a Small Acinetobacter Plasmid Carrying an oriT Transfer Origin by Conjugative RepAci6 Plasmids. *Plasmid* **2019**, *103*, 36–44. [CrossRef] [PubMed]
34. Hamidian, M.; Ambrose, S.J.; Hall, R.M. A Large Conjugative *Acinetobacter baumannii* Plasmid Carrying the Sul2 Sulphonamide and strAB Streptomycin Resistance Genes. *Plasmid* **2016**, *87–88*, 43–50. [CrossRef] [PubMed]
35. Uechi, K.; Tohya, M.; Tada, T.; Tome, T.; Takahashi, A.; Kinjo, T.; Maeda, S.; Kirikae, T.; Fujita, J. Emergence of a Multidrug-Resistant Plasmid Encoding Bla NDM-1, Bla OXA-420 and armA in a Clinical Isolate of Acinetobacter Variabilis in Japan. *J. Med. Microbiol.* **2021**, *70*. [CrossRef] [PubMed]
36. Tobin, L.A.; Jarocki, V.M.; Kenyon, J.; Drigo, B.; Donner, E.; Djordjevic, S.P.; Hamidian, M. Genomic Analysis of Diverse Environmental *Acinetobacter* Isolates Identifies Plasmids, Antibiotic Resistance Genes, and Capsular Polysaccharides Shared with Clinical Strains. *Appl. Environ. Microbiol.* **2024**, *90*, e0165423. [CrossRef] [PubMed]
37. Landman, D.; Quale, J.M.; Mayorga, D.; Adedeji, A.; Vangala, K.; Ravishankar, J.; Flores, C.; Brooks, S. Citywide Clonal Outbreak of Multiresistant *Acinetobacter baumannii* and *Pseudomonas aeruginosa* in Brooklyn, NY: The Preantibiotic Era Has Returned. *Arch. Intern. Med.* **2002**, *162*, 1515–1520. [CrossRef] [PubMed]
38. Ayswarya, K.; Ibrahim, R.; Veetilvalappil, V.V.; Bhat, N.B.; Aranjani, J.M. Virulence Arsenal of *Acinetobacter baumannii*: Mechanisms Driving Persistence and Resistance. *Arch. Microbiol.* **2026**, *208*, 162. [CrossRef] [PubMed]
39. Garcillán-Barcia, M.P.; de la Cruz, F.; Rocha, E.P.C. The Extended Mobility of Plasmids. *Nucleic Acids Res.* **2025**, *53*, gkaf652. [CrossRef] [PubMed]